



Membrane solid phase microextraction with alumina hollow fiber on line coupled with ICP-OES for the determination of trace copper, manganese and nickel in environmental water samples

Chao Cui, Man He, Bin Hu*

Key Laboratory of Analytical Chemistry for Biology and Medicine (Ministry of Education), Department of Chemistry, Wuhan University, Wuhan 430072, China

ARTICLE INFO

Article history:

Received 4 November 2010
Received in revised form 6 January 2011
Accepted 10 January 2011
Available online 15 January 2011

Keywords:

Membrane solid phase microextraction
Alumina hollow fiber
Cu, Mn and Ni
Environmental water
ICP-OES

ABSTRACT

A novel alumina hollow fiber was synthesized by sol-gel template method and was characterized by scanning electron microscopy, N_2 adsorption technique and X-ray diffraction. With the use of prepared alumina hollow fiber as extraction membrane, a new method of flow injection (FI)-membrane solid phase microextraction (MSPME) on-line coupled to inductively coupled plasma-optical emission spectrometry (ICP-OES) was developed for simultaneous determination of trace metals (Cu, Mn and Ni) in environmental water samples. The adsorption capacities of the alumina hollow fiber for Cu, Mn and Ni were found to be 6.6, 8.7 and 13.3 $mg\ g^{-1}$, respectively. With a preconcentration factor of 10, the limits of detection (LODs) for Cu, Mn and Ni were found to be 0.88, 0.61 and 0.38 $ng\ mL^{-1}$, respectively, and the relative standard deviations (RSDs) were ranging from 6.2 to 7.9% ($n=7$, $c=10\ ng\ mL^{-1}$). To validate the accuracy, the proposed method was applied to the analysis of certified reference material GSBZ50009-88 environmental water and the determined values are in good agreement with the certified values. The developed method was also employed for the analysis of Yangtze River water and East Lake water, and the recoveries for the spiked samples were in the range of 87.4–110.2%.

© 2011 Elsevier B.V. All rights reserved.

1. Introduction

Membrane separation is a highly efficient separation technology and has been widely used in hemodialysis, water desalination, natural gas treatment, wastewater purification, blood oxygenator, etc. [1,2]. One of the most common modes for its application is to separate analytes in different sizes by the nano/macro pores of the membrane, and the other is to make full use of its adsorption characteristics. Membrane based solid phase microextraction (MSPME) involving membrane as the adsorption material integrates sampling, extraction and concentration into a single step and inherits the advantages of solid phase microextraction (SPME) and membrane separation [3].

In the development of MSPME, exploration of novel extraction membrane with excellent performance has attracted great interest for that the employed extraction membrane is one of the key factors that determine the sensitivity and the selectivity of the analytical method [4,5]. Organic film and polymer film, due to their advantages of flexibility, high permeability, low density, good film-forming and low-cost, have been widely used in the analysis of drug and pesticide residues in real samples [3,6,7]. Compared with

common organic membrane, inorganic membrane exhibits much better resistance to strong acid/alkaline and high temperature [8], resulting in an increasing interest on the synthesis and application of various inorganic oxide membranes, such as titania [9,10], alumina [11–14], silica [15,16], zirconia [17–19]. Porous anodic alumina membrane has been widely used in catalysis [20], separation technology [21], optoelectronics [22]. Various types of alumina film can be synthesized through chemical vapor deposition, anodic oxidation, solid particles sintering, phase transfer/sintering [23] and template method [12–14]. Compared with other methods, template method is easy to operate and the topography of the obtained product can be easily controlled [24]. Liao and Shi's group synthesized mesoporous alumina membrane by using collagen membrane as a template and the synthetic process and mechanism have been investigated [13]. When cotton was used as the template, the prepared alumina film is almost identical to its template in terms of morphology [14]. Recently, polypropylene hollow fibers have been applied as the template for the synthesis of zirconia hollow fiber [17,19] and titania hollow fiber [10]. The obtained zirconia and titania fibers have the characteristics of porous membrane structure, uniform textural pores, and high surface area, which make them good alternatives for MSPME adsorption material. Based on our literatures survey, hitherto, MSPME based on alumina hollow fiber for trace elemental analysis has not been reported.

* Corresponding author. Tel.: +86 27 68752162; fax: +86 27 68754067.
E-mail address: binhu@whu.edu.cn (B. Hu).

Table 1
Optimized operating conditions for ICP-OES.

RF generator power (W)	1150
Frequency of RF generator (MHz)	27.12
Coolant gas flow rate (L min ⁻¹)	14
Auxiliary gas (L min ⁻¹)	0.5
Plasma gas (L min ⁻¹)	0.6
Observation height (mm)	15
Max integration times (s)	30
Analytical wavelength (nm)	
Cu	324.754
Mn	257.610
Ni	341.476

Cu, Mn and Ni are the essential trace elements for human being, while excessive intake of such metals would endanger our health. With so much natural and human activities, such as crustal movement, industrial and agricultural sewage discharge, heavy metals contamination has become a significant threat to the ecosystem and human health [25,26]. Consequently, the development of reliable methods for the removal and determination of such heavy metals in environmental samples is of particular significance.

The aim of this work was to prepare a new alumina hollow fiber membrane by using polypropylene hollow fiber as the template, and investigate the adsorption behaviors of Cu, Mn and Ni on the self-prepared material. Based on these investigations, a new method of flow injection (FI)-MSPME-ICP-OES was proposed for the determination of target metal ions in environmental water samples.

2. Experimental

2.1. Apparatus

Magnetic mixer (7312-I, Shanghai Standard Mode Factory, Shanghai) was used in the synthesis procedure. Vacuum drying oven (DZG-6020, Shanghai Senxin Instrument Factory, Shanghai) and X2-6-13 muffle furnace (Yingshan Yahua Instrument Factory, Hubei, China) were used to achieve the desired temperature. The synthesized alumina hollow fiber was characterized by X-ray diffractometer (Lab X-3000, Shimadzu, Japan) and Scanning Electron Microscope (Hitachi modal X-650, Tokyo, Japan). Nitrogen adsorption/desorption experiments were carried out with a Beckman Coulter (Miami, FL, USA) SA 3100 Plus surface area and pore size analyzer. The specific surface area values were calculated according to the Brunauer–Emmett–Teller equation. The pore parameters (pore volumes and pore diameters) were evaluated from the desorption branches of isotherms based on the Barrett–Joyner–Halenda model.

Intrepid XSP ICP-OES (Thermo, Waltham, MA, USA) with a concentric model nebulizer and a cinnabar model spray chamber was used for the determination of target metal ions, and the optimum operation conditions are summarized in Table 1. The pH values of aqueous solution were adjusted by a Mettler Toledo 320-S pH meter (Mettler Toledo Instruments Co. Ltd., Shanghai, China) supplied with a combined electrode. An IFIS-C flow injection system (Ruimai Tech. Co. Ltd., Xi'an, China) and a PTFE tubing (0.6 mm i.d., 10 cm length) packed with alumina hollow fiber were used in the on-line separation/preconcentration process. A minimum length of PTFE tubing (0.4 mm i.d.) was used for all connections in order to minimize the dead volume. The Accurel Q3/2 polypropylene hollow fiber membrane (600 μm i.d., 200 μm wall thickness, 0.2 μm pore size) was purchased from Membrane GmbH (Wuppertal, Germany).

2.2. Standard solution and reagents

The stock solutions (1 g L⁻¹) of Mn(II), Ni(II) and Cu(II) were prepared by dissolving appropriate amounts of MnSO₄, NiSO₄·(NH₄)₂SO₄·6H₂O and CuSO₄·5H₂O (analytical reagent grade, The First Reagent Factory, Shanghai, China) in high purity water, respectively. Working solutions were prepared daily by appropriate dilutions of stock solutions. AlCl₃ (analytical reagent grade) was also purchased from the First Reagent Factory, Shanghai, China. The employed HNO₃, HCl, CH₃CH₂OH and NH₃·H₂O were of analytical reagent grade and all other reagents used were of spec pure grade or analytical reagent grade. High purity water obtained by Repure system (MRM-III-20, Origin of High Purity Technology Co., Ltd., Wuhan, China) was used throughout the experiment.

2.3. Synthesis of alumina hollow fiber

2.3.1. Preparation of alumina sol

Alumina sol was prepared according to the procedure described in Refs. [27,28]. Briefly, 1.33 g AlCl₃ and two drops of 1 mol L⁻¹ HNO₃ were added into 10 g ethanol with stirring for 30 min. The resulting sol solutions were then aged at 70 °C in the drying oven for 2 days.

2.3.2. Preparation of alumina hollow fiber

Polypropylene hollow fibers were ultrasonicated in acetone for 15 min, then removed out and dried in the air. For coating, the dried polypropylene hollow fibers were immersed in the above-prepared alumina sol, followed by a drying procedure with careful temperature control at 60 °C for 4 h. Then, the above immersion and drying process were repeated for several times, resulting in alumina coated-polypropylene hollow fibers. Finally, the coated hollow fibers were heated from room temperature to 800 °C at 2 °C/min and maintained for 3 h to remove the polypropylene template and crystallize the alumina.

2.4. Preparation of micro-column

10 mg of alumina hollow fiber was filled into PTFE soft tubing (0.6 mm i.d.) plugged with PTFE hard tubing (0.4 mm i.d.) at both ends. Before use, 1.0 mol L⁻¹ HNO₃ and high purity water were passed through the column in sequence to remove possible impurities. Then, the column was conditioned to the desired pH with 0.1 mol L⁻¹ NH₄NO₃ buffer solution.

2.5. Sample preparation

Water samples, including river water and lake water, were collected from Yangtze River and East Lake (Wuhan, China), respectively. Immediately after sampling, water samples were filtered through a 0.45 μm membrane (Tianjing Jinteng Instrument Factory, Tianjin, China) and adjusted to pH 8.5 with 0.01 mol L⁻¹ HNO₃ and 0.01 mol L⁻¹ NH₃·H₂O. After that, the sample solutions were analyzed immediately.

Certified reference material GSBZ50009-88 environmental water was provided by the Institute for Environmental Reference Materials, Ministry of Environmental Protection of China, Beijing, China. Prior to use, the ampoule was broken carefully at the neck and 10 mL of the sample was pipetted into 250 mL volumetric flask and made to the calibrate with high purity water according to the instructions of the supplier. The sample was further diluted and adjusted to pH 8.5 with 0.01 mol L⁻¹ HNO₃ and 0.01 mol L⁻¹ NH₃·H₂O prior to analysis.

High purity water without analytes addition was employed as the blank and subjected to the same procedure described above.

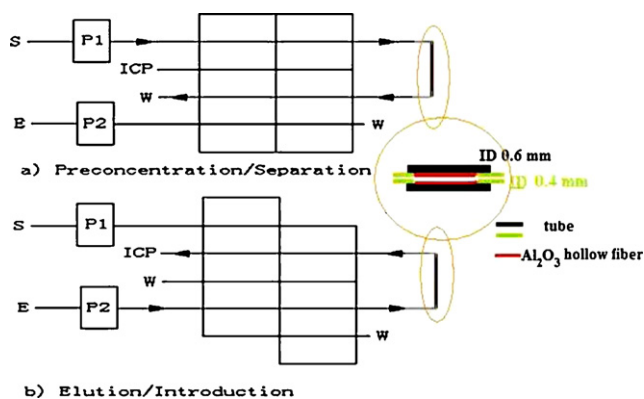


Fig. 1. FI manifold and operation for on-line preconcentration/separation and ICP-OES determination. (a) Preconcentration/separation step, (b) elution/introduction step. For details see text. S, sample; E, elution; W, waste; P1, P2, peristaltic pumps; ICP, ICP torch.

2.6. General procedure

The operation sequence of the FI on-line column preconcentration and ICP-OES determination is shown in Fig. 1. In separation/preconcentration step, pump P1 was activated, so that the sample was drawn through the column and the effluent was led to the waste. And in elution step, pump P2 was activated and the eluent was propelled through the column reversely, the eluting solution was then introduced into the ICP-OES for determination.

3. Results and discussion

3.1. Characterization of alumina hollow fiber

The self-prepared alumina hollow fiber was characterized by powder X-ray diffraction (XRD), scanning electron microscopy (SEM), and low-temperature nitrogen adsorption/desorption measurements.

3.1.1. X-ray diffraction analysis

Alumina has different crystal forms including $\text{Al}(\text{OH})_3$, $\text{AlO}(\text{OH})$, $\gamma\text{-Al}_2\text{O}_3$, $\delta\text{-Al}_2\text{O}_3$, $\theta\text{-Al}_2\text{O}_3$, $\alpha\text{-Al}_2\text{O}_3$, and so on. Among them, $\gamma\text{-Al}_2\text{O}_3$ shows excellent resistance to strong acid/alkaline and high temperature, and other special characteristics, resulting in an application potential in catalyst and solid phase extraction [29]. Fig. 2 shows XRD patterns of alumina calcinated at different temperatures, and an obvious crystal forms transformation was observed.

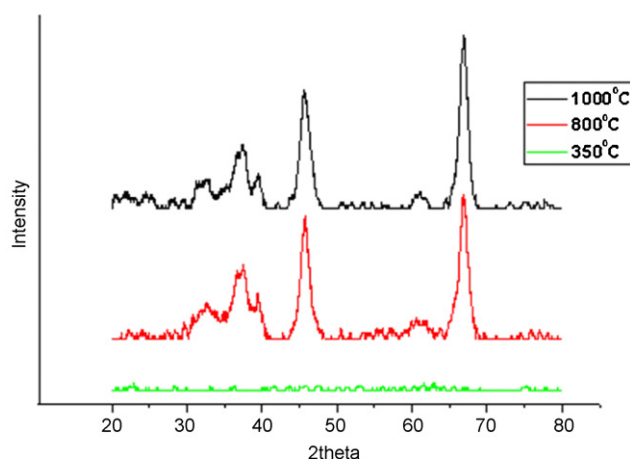


Fig. 2. XRD spectra of Al_2O_3 hollow fiber at different temperatures.

Table 2
Pore structure parameters based on measurement of nitrogen adsorption/desorption.

Material	Surface area (m^2/g)	Pore volume (mL/g)	Pore size (nm)
Polypropylene hollow fiber	26.1	0.09	21.3
Alumina hollow fiber	81.2	0.05	6

The characteristic peaks of $\gamma\text{-Al}_2\text{O}_3$ appeared obviously at 37.6° , 45.8° and 66.8° (2θ) when the calcination temperature is above 800°C , which accords with that reported in Ref. [14]. In this work, $\gamma\text{-Al}_2\text{O}_3$ hollow fibers were employed as the extraction material, therefore, calcination at 800°C for 3 h was selected for the preparation of alumina hollow fibers.

3.1.2. Scanning electron microscopy analysis

Fig. 3 shows the SEM images of alumina hollow fiber and polypropylene hollow fiber at different magnifications and different view angles. From the cross-sectional image (Fig. 3a) and longitudinal image (Fig. 3b) of the alumina hollow fiber, it can be seen that the inner diameter of alumina hollow fiber is about $350\ \mu\text{m}$ and its thickness is about $100\ \mu\text{m}$. Compared with polypropylene hollow fiber (i.d. $600\ \mu\text{m}$, thickness $200\ \mu\text{m}$), the self-prepared alumina hollow fiber displayed $\sim 40\%$ radial shrinkage. While for the surface topography, both of them present porous structure (Fig. 3c and d). With much greater magnification, nanopores in different sizes were observed in the textural image of alumina hollow fiber (Fig. 3e), which is quite different from that observed in polypropylene hollow fiber (Fig. 3f). It should be pointed out that these nanopores in the self-prepared alumina hollow fibers will lead to an enhanced surface area and fast mass transfer for the analytes during the extraction process.

3.1.3. Pore structure parameters

Based on nitrogen adsorption/desorption experiments, the pore structure parameters of polypropylene hollow fiber and alumina hollow fiber were investigated and the results are listed in Table 2. As can be seen, the surface area of alumina hollow fiber is twice larger than that of polypropylene hollow fiber and alumina hollow fiber has much smaller average pore size than polypropylene hollow fiber.

3.2. Optimization of MSPME conditions

3.2.1. Effect of pH

The pH value plays an important role in the adsorption of different metal ions on the oxide surfaces. In order to investigate the effect of pH on the adsorption percentage of target analytes, sample solutions were adjusted to pH 2–9 and then subjected to the operation procedure as described in Section 2.6. Fig. 4 is the effect of pH on the adsorption percentage of $\text{Cu}(\text{II})$, $\text{Mn}(\text{II})$ and $\text{Ni}(\text{II})$. As can be seen, in the pH range of 2–8, the adsorption percentage of target analytes was obviously increased with the increase of pH. When pH is above 8, the adsorption percentage of target analytes was maintained at around 95%. The above results could be explained by the following facts. The surface of alumina hollow fiber is positively charged when the pH is lower than the isoelectric point (~ 8) of alumina, resulting in an electrostatic repulsion for the target metal ions. When pH is above the isoelectric point, negatively charged alumina hollow fiber attracted target ions and led to an enhancement of the adsorption efficiency. In subsequent experiment, pH 8.5 was used for simultaneous adsorption of Cu, Mn and Ni.

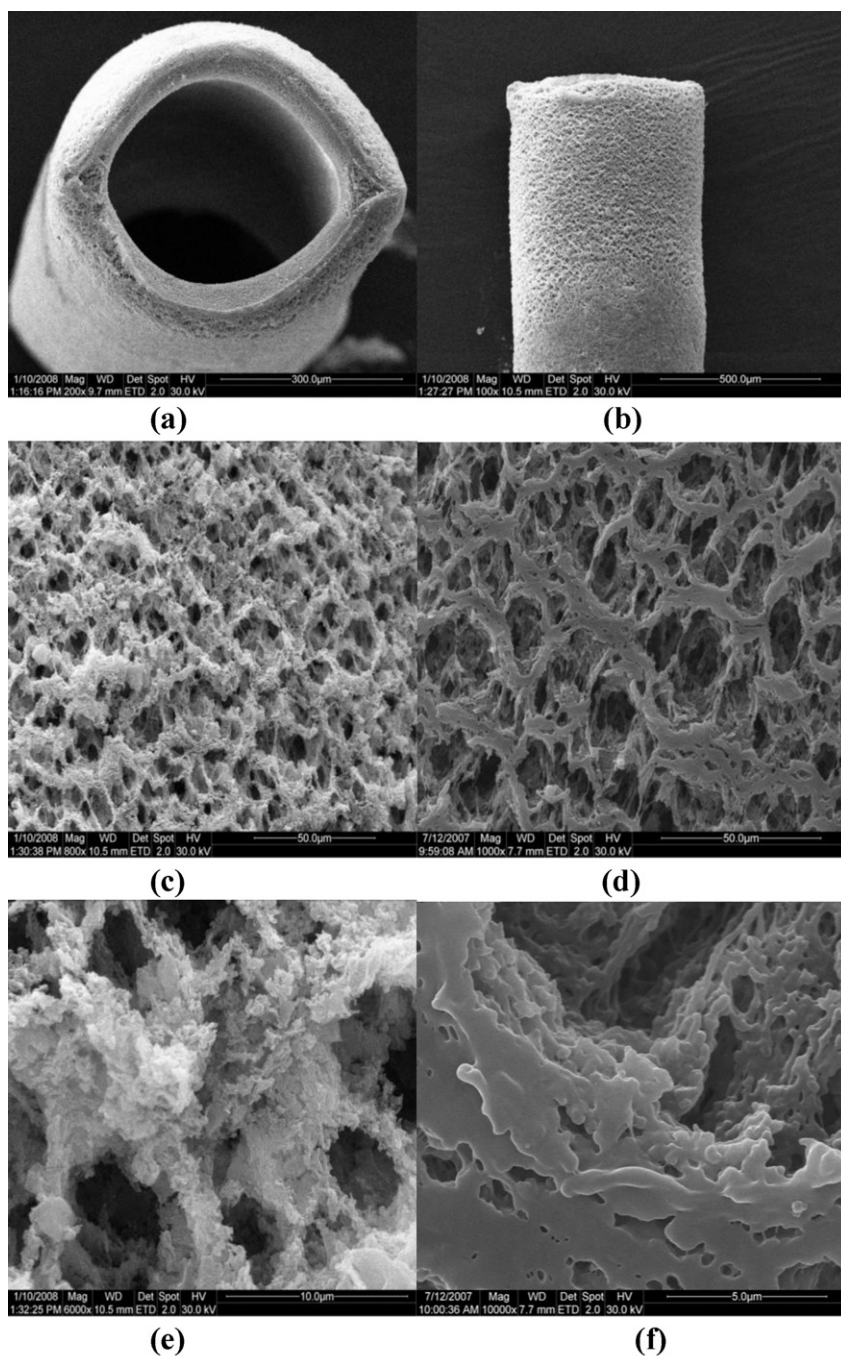


Fig. 3. SEM images of Al_2O_3 and polypropylene hollow fiber: (a) cross-sectional image of Al_2O_3 hollow fiber; (b) longitudinal image of Al_2O_3 hollow fiber; (c) textural image of Al_2O_3 hollow fiber; (d) textural image of polypropylene hollow fiber; (e) nanopores of Al_2O_3 hollow fiber; (f) fibrous structure of polypropylene hollow fiber.

3.2.2. Effects of sample flow rate and sample volume

The effect of flow rate of sample solutions in the range of $0.1\text{--}1.4\text{ mL min}^{-1}$ on the adsorption percentage of target analytes was examined and the results are shown in Fig. 5. It was found that Mn, Ni and Cu could be adsorbed quantitatively when the sample flow rate was in the range of $0.1\text{--}0.3\text{ mL min}^{-1}$, while the adsorption percentage was decreased with a further increase of the sample flow rate. For further experiments, a sample flow rate of 0.3 mL min^{-1} was applied.

In order to increase the enrichment factor as possible, large volume of sample solution is favorable. For this purpose, the effect of sample volume on the recovery of target analytes was investigated and the results are shown in Fig. 6. As can be seen, no obvious influ-

ence of sample volume on the recovery of the target analytes was observed in the range of $1\text{--}20\text{ mL}$. However, it should be pointed out that 20 mL of sample loading would take much more time and result in a low sampling frequency. To trade off the enrichment factor and analytical speed, a sample volume of 3 mL was used in the experiment.

3.2.3. Optimization of elution conditions

As can be seen from Fig. 4, the adsorption of target metal ions was negligible at $\text{pH} < 2$. Thereby HCl was used as the eluent for the elution of the target analytes and the effect of HCl concentration in the range of $1\text{--}3\text{ mol L}^{-1}$ on the recovery of target analytes was investigated. As shown in Fig. 7, the recovery of Mn, Ni and

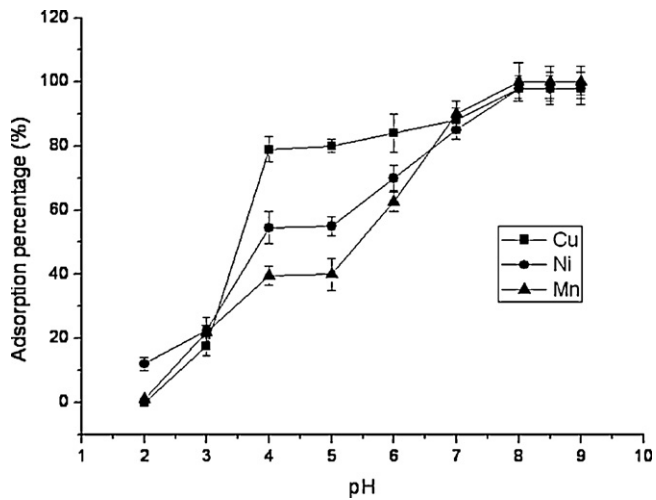


Fig. 4. Effect of pH on the adsorption percentage of Cu^{2+} , Mn^{2+} and Ni^{2+} on Al_2O_3 fiber. Conditions: sample volume: 3 mL; the concentration of target analytes: $0.2 \mu\text{g mL}^{-1}$.

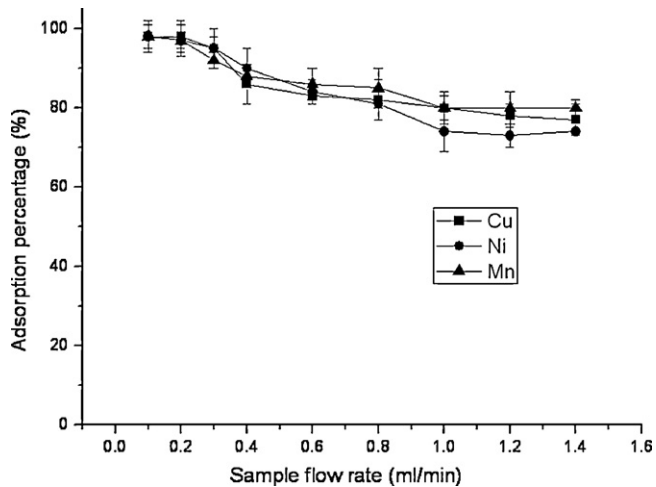


Fig. 5. Effect of sample flow rate on the adsorption percentage of Cu^{2+} , Mn^{2+} and Ni^{2+} on Al_2O_3 fiber. Conditions: sample volume: 3 mL; the concentration of target analytes: $0.2 \mu\text{g mL}^{-1}$; pH = 8.5.

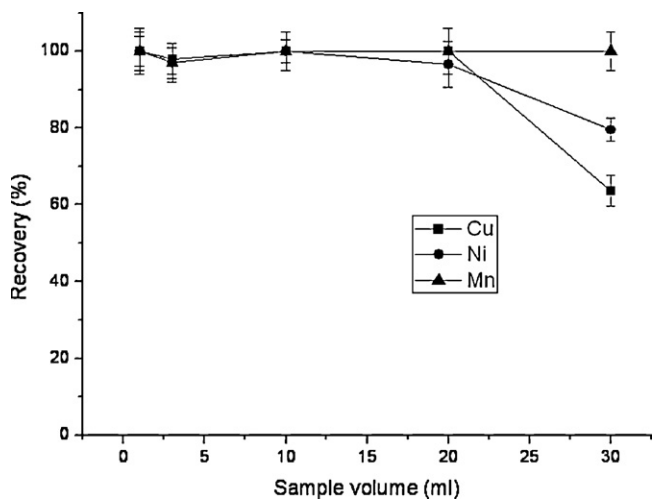


Fig. 6. Effect of sample volume on the recovery of Cu^{2+} , Mn^{2+} and Ni^{2+} on Al_2O_3 fiber conditions: the concentration of target analytes: $0.2 \mu\text{g mL}^{-1}$; pH = 8.5; sample flow rate: 0.3 mL min^{-1} .

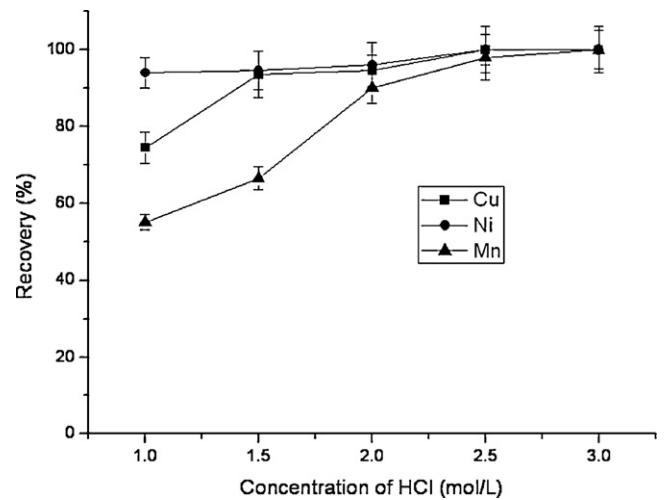


Fig. 7. Effect of HCl concentration on the recovery of Cu^{2+} , Mn^{2+} and Ni^{2+} on Al_2O_3 fiber. Conditions: sample volume: 3 mL; the concentration of target analytes: $0.2 \mu\text{g mL}^{-1}$; pH = 8.5; sample flow rate: 0.3 mL min^{-1} .

Cu was increased continuously with HCl concentration increasing from 1 mol L^{-1} to 2.5 mol L^{-1} , and maintained constant with the further increase of HCl concentration. For further experiments, 2.5 mol L^{-1} HCl was selected as the eluent.

The effect of elution flow rate on the recovery of target analytes was examined with the flow rate varying in the range of $0.2\text{--}1.2 \text{ mL min}^{-1}$. It was found that Mn, Ni and Cu could be recovered quantitatively when the elution flow rate was in the range of $0.2\text{--}0.4 \text{ mL min}^{-1}$, while the recovery was obviously decreased with a further increase of the elution flow rate. Additionally, the effect of elution volume on the recovery of target analytes was investigated and the results are shown in Fig. 8. As can be seen, the recovery of Mn, Ni and Cu was increased with the increase of elution volume from 0.1 to 0.3 mL and maintained constant in the elution volume range of 0.3–0.5 mL. In the subsequent experiment, $0.3 \text{ mL } 2.5 \text{ mol L}^{-1}$ HCl was used to recover the target analytes at a flow rate of 0.3 mL min^{-1} .

3.2.4. Adsorption capacity and regeneration

Adsorption capacity is an important factor to evaluate the performance of the solid phase extraction material, since it determines

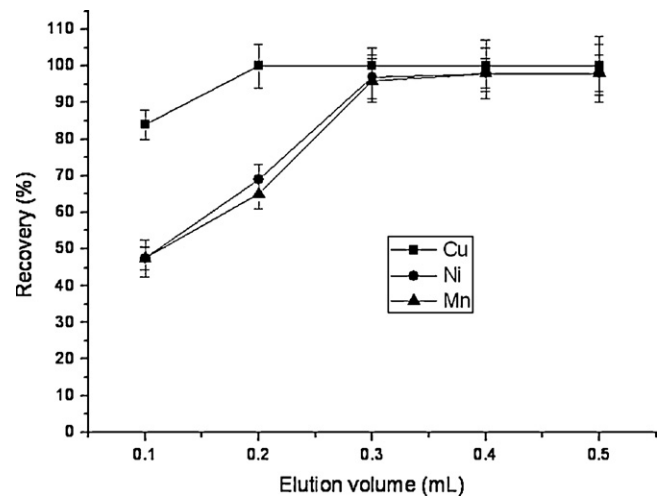


Fig. 8. Effect of elution volume on the recovery of Cu^{2+} , Mn^{2+} and Ni^{2+} on Al_2O_3 fiber. Conditions: sample volume: 3 mL; the concentration of target analytes: $0.2 \mu\text{g mL}^{-1}$; pH = 8.5; sample flow rate: 0.3 mL min^{-1} ; eluent: 2.5 mol L^{-1} HCl; elution flow rate: 0.3 mL min^{-1} .

Table 3
Comparison of adsorption capacities (mg g^{-1}).

Element	Sorbents						
	Al ₂ O ₃ hollow fiber	Nanometer sized Al ₂ O ₃	Mesoporous TiO ₂	Nanometer sized TiO ₂	High surface area ZrO ₂	Pyrogallol Immobilized Amberlite XAD-2	Multiwalled carbon nanotubes
	This work	[29]	[31]	[32]	[33]	[34]	[35]
Cu	6.6	13.3	8.1	6.9	7.9	4.5	–
Mn	8.7	15.7	22.3	2.1	6.2	4.5	4.9
Ni	13.3	12.2	8.6	2.0	5.6	4.1	6.9

Table 4
Effect of coexisting ions on the adsorption of analytes.

Coexisting	Tolerance limit of ions (mg L^{-1})
K ⁺	3000
Na ⁺	5000
Ca ²⁺ , Mg ²⁺	2000
Fe ³⁺	50
Zn ²⁺	10
Cl ⁻	3500
SO ₄ ²⁻	5000
CH ₃ COO ⁻	20
CO ₃ ²⁻	500

how much alumina hollow fiber is required to quantitatively concentrate target analytes from a given solution. Based on the method recommended by Maquleira et al. [30], the adsorption capacities of the self-prepared alumina hollow fiber for Cu, Mn and Ni were investigated and the results are listed in Table 3. For comparison, Table 3 also showed the adsorption capacity data of other nanometer sized materials and mesoporous oxides reported in the literatures [29,31–35]. As can be seen, the adsorption capacity of the alumina hollow fiber for the target metals ions is higher than that obtained by multiwall carbon nanotubes [35] and Pyrogallol Immobilized Amberlite XAD-2 [34], comparable with that obtained by nanometer-sized ZrO₂ [33] and TiO₂ [32] and mesoporous TiO₂ [31] adsorbents, but smaller than that reported in Ref. [29].

Regeneration is another important characteristic to evaluate the performance of employed adsorption material. By performing the adsorption and desorption repeatedly, it was found that 2.5 mol L⁻¹ HCl could regenerate the alumina hollow fiber and the alumina hollow fiber could be reused for more than 20 times without obvious loss of analytical performance.

3.2.5. Effects of coexisting ions

The interference induced by common coexisting ions, such as K⁺, Na⁺, Ca²⁺, Mg²⁺, Fe³⁺, and Zn²⁺, on the preconcentration and determination of target analytes ($0.2 \mu\text{g mL}^{-1}$) were examined under the optimum conditions, and the results are summarized in Table 4. As can be seen, up to $3000 \mu\text{g mL}^{-1}$ of K⁺, $5000 \mu\text{g mL}^{-1}$ of Na⁺, $2000 \mu\text{g mL}^{-1}$ Ca²⁺ and Mg²⁺, $50 \mu\text{g mL}^{-1}$ of Fe³⁺, $10 \mu\text{g mL}^{-1}$ of Zn²⁺, $3500 \mu\text{g mL}^{-1}$ of Cl⁻, $5000 \mu\text{g mL}^{-1}$ of SO₄²⁻, $20 \mu\text{g mL}^{-1}$ of CH₃COO⁻ and $500 \mu\text{g mL}^{-1}$ of CO₃²⁻ had no significant interfer-

Table 6
Analytical results of Cu, Mn and Ni in water samples (mean \pm SD, $n = 3$).

Element	Yangtze river			Eastlake		
	Added (ng mL^{-1})	Found (ng mL^{-1})	Recovery (%)	Added (ng mL^{-1})	Found (ng mL^{-1})	Recovery (%)
Cu	0	3.3 ± 0.4	–	0	3.0 ± 0.4	–
	10	14.3 ± 0.8	110.2	5	7.9 ± 0.8	98.6
Mn	0	2.4 ± 0.3	–	0	5.0 ± 0.7	–
	10	12.4 ± 1.8	100.5	5	9.8 ± 0.6	96.7
Ni	0	7.7 ± 0.9	–	0	5.5 ± 0.9	–
	10	16.1 ± 1.7	87.4	5	10.0 ± 1.0	90.3

Table 5
Analytical results of certified reference material (mean \pm SD, $n = 3$).

Element	GSBZ50009-88	
	Found (mg L^{-1})	Certified (mg L^{-1})
Cu	1.44 ± 0.230	1.49 ± 0.116
Mn	n.d.	–
Ni	0.85 ± 0.043	0.886 ± 0.036

n.d.: not detected.

ences on the preconcentration and determination of target metal ions, indicating an application potential of the proposed method in real sample analysis [36].

3.3. Analytical performance

Under the optimized operating conditions, a preconcentration time of 10 min and elution time of 1 min resulted in a sampling frequency of 5 h^{-1} . The detection limits (evaluated as the concentration corresponding to three times the standard deviation of 11 runs of the blank solution) obtained by on-line FI-MSPME-ICP-OES system were 0.88 , 0.61 and 0.38 ng mL^{-1} for Cu, Mn and Ni, respectively. The reproducibility of the proposed method was also evaluated and the relative standard deviations (RSDs) ($n = 7$, $c = 10 \text{ ng mL}^{-1}$) were calculated to be 7.9, 6.2 and 7.2% for Cu, Mn and Ni, respectively.

3.4. Sample analysis

The accuracy of the proposed method was validated by determining target metal ions in the certified reference material GSBZ50009-88 environmental water, and the analytical results are given in Table 5. As can be seen, the determined values were in good agreement with the certified values.

The proposed method was also applied to the determination of target analytes in real water samples including Yangtze River water and East Lake water. The analytical results and the recoveries for the spiked samples are given in Table 6. It can be seen that the recoveries for the spiked samples are between 87.4 and 110.2%.

4. Conclusions

Alumina hollow fiber was successfully synthesized by sol-gel method with template process and characterized by various techniques. The as-synthesized alumina hollow fiber was featured with porous structure, large surface area and high adsorption capacity and its application potential as a novel adsorption material for membrane solid phase microextraction (MSPME) of the target metal ions has been demonstrated by on line FI-MSPME-ICP-OES determination of trace Cu, Mn and Ni in environmental water samples.

Acknowledgements

Financial supports from the Science Fund for Creative Research Groups of NSFC (Nos. 20621502, 20921062) and MOE of China (NCET-04-0658) are gratefully acknowledged.

References

- [1] H. Strathmann, Membrane separation processes: current relevance and future opportunities, *AIChE J.* 47 (2001) 1077–1087.
- [2] D. Paul, K. Ohlrogge, Membrane separation processes for clean production, *Environ. Prog. Sust. Energy* 17 (1998) 137–141.
- [3] R.Q. Yang, W.L. Xie, Determination of cannabinoids in biological samples using a new solid phase micro-extraction membrane and liquid chromatography-mass spectrometry, *Forensic Sci. Int.* 162 (2006) 135–139.
- [4] S.H. Zhan, D.R. Chen, X.L. Jiao, H.T. Cai, Long TiO₂ fibers with mesoporous walls: sol-gel electrospun fabrication and photocatalytic properties, *J. Phys. Chem. B* 110 (2006) 11199–11204.
- [5] J.S. Li, L.J. Wang, Y.X. Hao, X.D. Liu, X.Y. Sun, Preparation and characterization of Al₂O₃ hollow fiber membranes, *J. Membr. Sci.* 256 (2005) 1–6.
- [6] R.Q. Yang, W.L. Xie, Preparation and usage of a new solid phase micro-extraction membrane, *Forensic Sci. Int.* 139 (2004) 177–181.
- [7] C. Basheer, V. Suresh, R. Renu, H.K. Lee, Development and application of polymer-coated hollow fiber membrane microextraction to the determination of organochlorine pesticides in water, *J. Chromatogr. A* 1033 (2004) 213–220.
- [8] X.Y. Tan, S.M. Liu, K. Li, Preparation and characterization of inorganic hollow fiber membranes, *J. Membr. Sci.* 188 (2001) 87–95.
- [9] S. Kobayashi, K. Hanabusa, N. Hamasaki, M. Kimura, H. Shirai, S. Shinkai, Preparation of TiO₂ hollow-fibers using supramolecular assemblies, *Chem. Mater.* 12 (2000) 1523–1525.
- [10] J. Li, H.Y. Qi, Y.P. Shi, Applications of titania and zirconia hollow fibers in sorptive microextraction of N,N-dimethylacetamide from water sample, *Anal. Chim. Acta* 651 (2009) 182–187.
- [11] S.M. Liu, K. Li, R. Hughes, Preparation of porous aluminium oxide (Al₂O₃) hollow fibre membranes by a combined phase-inversion and sintering method, *Ceram. Int.* 29 (2003) 875–881.
- [12] M. Llusar, L. Pícol, C. Roux, J.L. Pozzo, C. Sanchez, Templated growth of alumina-based fibers through the use of anthracenic organogelators, *Chem. Mater.* 14 (2002) 5124–5133.
- [13] D.H. Deng, R. Tang, X.P. Liao, B. Shi, Using collagen fiber as a template to synthesize hierarchical mesoporous alumina fiber, *Langmuir* 24 (2008) 368–370.
- [14] T.X. Fan, B.H. Sun, J.J. Gu, D. Zhang, L.W.M. Lau, Biomorphic Al₂O₃ fibers synthesized using cotton as bio-templates, *Scripta Mater.* 53 (2005) 893–897.
- [15] T.A. Peters, J. Fontalvo, M.A.G. Vorstman, N.E. Benes, R.A. van Dam, Z.A.E.P. Vroon, E.L.J. van Soest-Vercammen, J.T.F. Keurentjes, Hollow fiber microporous silica membranes for gas separation and pervaporation synthesis performance and stability, *J. Membr. Sci.* 248 (2005) 73–80.
- [16] J. Li, H.F. Zhang, Y.P. Shi, Application of SiO₂ hollow fibers for sorptive microextraction and gas chromatography-mass spectrometry determination of organochlorine pesticides in herbal matrices, *Anal. Bioanal. Chem.* 398 (2010) 1501–1508.
- [17] L. Xu, H.K. Lee, Zirconia hollow fiber: preparation, characterization, and microextraction application, *Anal. Chem.* 79 (2007) 5241–5248.
- [18] H.Y. Liu, X.Q. Hou, X.Q. Wang, Y.L. Wang, D. Xu, C. Wang, W. Du, M.K. Lu, D.R. Yuan, Fabrication of high-strength continuous zirconia fibers and their formation mechanism study, *J. Am. Ceram. Soc.* 87 (2004) 2237–2241.
- [19] J. Li, H.Y. Qian, Y.P. Shi, Determination of melamine residues in milk products by zirconia hollow fiber sorptive microextraction and gas chromatography-mass spectrometry, *J. Chromatogr. A* 1216 (2009) 5467–5471.
- [20] L. Zhou, Y. Guo, M. Yagi, M. Sakurai, H. Kameyama, Investigation of a novel porous anodic alumina plate for methane steam reforming: hydrothermal stability electrical heating possibility and reforming reactivity, *Int. J. Hydrogen Energy* 34 (2009) 844–858.
- [21] T. Yamashita, S. Kodama, T. Kemmei, M. Ohto, E. Nakayama, T. Muramoto, A. Yamaguchi, N. Teramae, N. Takayanagi, Separation of adenine, adenosine-5'-monophosphate and adenosine-5'-triphosphate by fluidic chip with nanometer-order diameter columns inside porous anodic alumina using an aqueous mobile phase, *Lab Chip* 9 (2009) 1337–1339.
- [22] Y.T. Pang, G.W. Meng, L.D. Zhang, W.J. Shan, X.Y. Gao, A.W. Zhao, Y.Q. Mao, Arrays of ordered Pb nanowires with different diameters in different areas embedded in one piece of anodic alumina membrane, *J. Phys.: Condens. Matter* 14 (2002) 11729–11736.
- [23] G.Z. Cao, D.W. Liu, Template-based synthesis of nanorod, nanowire, and nanotube arrays, *Adv. Colloid Interface Sci.* 136 (2008) 45–64.
- [24] C. Bae, H.J. Yoo, S. Kim, K. Lee, J.Y. Kim, M.M. Sung, H. Shin, Template-directed synthesis of oxide nanotubes: fabrication, characterization, and applications, *Chem. Mater.* 20 (2008) 756–767.
- [25] S.Y. Li, Z.F. Xu, X.L. Cheng, Q.F. Zhang, Dissolved trace elements and heavy metals in the Danjiangkou Reservoir, China, *Environ. Geol.* 55 (2008) 977–983.
- [26] G. Tamasi, R. Cini, Heavy metals in drinking waters from Mount Amiata (Tuscany, Italy). Possible risks from arsenic for public health in the Province of Siena, *Sci. Total Environ.* 327 (2004) 41–51.
- [27] P.D. Yang, D.Y. Zhao, D.I. Margolese, B.F. Chmelka, G.D. Stucky, Generalized syntheses of large-pore mesoporous metal oxides with semicrystalline frameworks, *Nature* 396 (1998) 152–155.
- [28] W.L. Hu, B. Hu, Z.C. Jiang, On-line preconcentration and separation of Co, Ni and Cd via capillary microextraction on ordered mesoporous alumina coating and determination by inductively coupled plasma mass spectrometry (ICP-MS), *Anal. Chim. Acta* 572 (2006) 55–62.
- [29] J. Yin, Z.C. Jiang, G. Chang, B. Hu, Simultaneous on-line preconcentration and determination of trace metals in environmental samples by flow injection combined with inductively coupled plasma mass spectrometry using a nanometer-sized alumina packed micro-column, *Anal. Chim. Acta* 540 (2005) 333–339.
- [30] A. Maqulelra, H.A.M. Elmahadi, R. Puchades, Immobilized cyanobacteria for on-line trace metal enrichment by flow injection atomic absorption spectrometry, *Anal. Chem.* 66 (1994) 3632–3638.
- [31] C.Z. Huang, Z.C. Jiang, B. Hu, Mesoporous titanium dioxide as a novel solid-phase extraction material for flow injection micro-column preconcentration on-line coupled with ICP-OES determination of trace metals in environmental samples, *Talanta* 73 (2007) 274–281.
- [32] P. Liang, Y.C. Qin, B. Hu, T.Y. Peng, Z.C. Jiang, Nanometer-size titanium dioxide microcolumn on-line preconcentration of trace metals and their determination by inductively coupled plasma atomic emission spectrometry in water, *Anal. Chim. Acta* 440 (2001) 207–213.
- [33] E. Vassileva, N. Furuta, Application of high-surface-area ZrO₂ in preconcentration and determination of 18 elements by on-line flow injection with inductively coupled plasma atomic emission spectrometry, *Fresenius J. Anal. Chem.* 370 (2001) 52–59.
- [34] M. Kumar, D.P.S. Rathore, A.K. Singh, Pyrogallol immobilized amberlite XAD-2: a newly designed collector for enrichment of metal ions prior to their determination by flame atomic absorption spectrometry, *Microchim. Acta* 137 (2001) 127–134.
- [35] P. Liang, Y. Liu, L. Guo, J. Zeng, H.B. Lu, Multiwalled carbon nanotubes as solid-phase extraction adsorbent for the preconcentration of trace metal ions and their determination by inductively coupled plasma atomic emission spectrometry, *J. Anal. Atom. Spectrom.* 19 (2004) 1489–1492.
- [36] Q. Liu, *Environmental Chemistry*, Chemical Industry Press, 2003.